Civil Engineering and Architecture 11(3): 1415-1423, 2023 http://www.hrpub.org
DOI: 10.13189/cea.2023.110324

Evaluation of a Braced Excavation by Numerical Method: A Case Study

Vahid Rostami[1,*], Zainuddin Md Yusoff[1], Zahraalsadat Eliaslankaran[1], Haslinda Nahazanan[1], Ehsan Mousavi[2]

[1]Department of Civil Engineering, Universiti Putra Malaysia, Serdang 43400, Selangor, Malaysia
[2]Faculty of Engineering, Kashan University, Iran

Received November 30, 2022; Revised January 10, 2023; Accepted February 10, 2023

Cite This Paper in the Following Citation Styles

(a): *[1] Vahid Rostami, Zainuddin Md Yusoff, Zahraalsadat Eliaslankaran, Haslinda Nahazanan, Ehsan Mousavi , "Evaluation of a Braced Excavation by Numerical Method: A Case Study," Civil Engineering and Architecture, Vol. 11, No. 3, pp. 1415 - 1423, 2023. DOI: 10.13189/cea.2023.110324.*

(b): *Vahid Rostami, Zainuddin Md Yusoff, Zahraalsadat Eliaslankaran, Haslinda Nahazanan, Ehsan Mousavi (2023). Evaluation of a Braced Excavation by Numerical Method: A Case Study. Civil Engineering and Architecture, 11(3), 1415 - 1423. DOI: 10.13189/cea.2023.110324.*

Abstract Approximately 18 by 22 by 100 meters in size, a braced excavation operation at the Mahallati station on Tehran's Metro Line 7 took over eleven consecutive phases. Due to the significant depth-to-width ratio, a PLAXIS plane-strain finite element analysis was carried out. The lateral wall of the braced cut excavation was supported with three types of struts in four different rows. Due to the excavation of the soil, the tension condition was changed and caused some displacements and instabilities; therefore, the horizontal and vertical displacement of the excavation was studied. The maximum horizontal displacements of 35.32 mm occurred in the lateral wall at the excavation surface, whereas the maximum vertical displacements of 35.00 mm occurred at the excavation's base. In all stages, the highest lateral wall deflection values were between 0.00018 and 0.0016 of the depth. The maximum ground surface settlement near the excavation was 22.41mm, approximately 0.67 times the maximum subsequent wall deflection. In each phase, the maximum ground surface settlement distance from the wall was almost equivalent to 0.4 times the excavation depth. The numerical modeling shows that Plaxis2D is an effective software for analyzing the excavation of a braced cut.

Keywords Braced Excavation, Finite Element, Ground Surface Settlement, PLAXIS, Wall Deflection

1. Introduction

Due to the city's fast economic development over the last two decades, Tehran (Iran) has undertaken a large number of deep excavation projects for high-rise structures and subterranean transit networks. In recent decades, braced excavation has replaced traditional excavation methods for building subterranean structures in all types of soil because of its lower cost and reduced reliance on specialized equipment. Basements, parking lots, commercial complexes, metro railways, and pumping stations are examples of the construction that often occur in urban settings, and all of them need braced excavation. On the one hand, this area's excavations are often deep and wide. On the other hand, while constructing a deep excavation, it is common practice to do so close to nearby structures and utilities.

Evaluation of the lateral wall deflection, magnitude of ground settlement, and distribution of ground movements in the vicinity of an excavated wall is an inherent component of urban excavation design. Calculating the profile of ground surface settlement surrounding an excavation becomes an important responsibility for protecting structures.

Braced excavations are a common example of a complicated soil structure interaction issue that may be modeled using the finite element method (FEM). Prediction techniques for excavation soil displacements have been studied for quite some time [1], [2]. Surface

settling and wall deformation are the goals of a wide variety of numerical techniques [3]–[5] and empirical approaches [1], [6]. In the finite element approach, predictions of ground surface settlements rely on soil strains and may be produced with certainty when soil strains are minimal [7]. Generally, predicting the ground surface settlement is tougher than wall deflection [4], [8], [9]. At the beginning of the excavation process, the maximum ground surface settlement usually happens very close and next to the wall for relatively small and large wall deflection, respectively [10]. On the basis of 300 case studies, there exists a correlation between maximum settlement and distance [2], and, apparently, when the excavation reaches fifty percent of its depth, the maximum ground surface settlement distance can be anticipated [10]. Peck discovered in 1969 that in soft clay, surface settling might extend laterally three to four times the excavated depth [5].

The excavation depth, the material characteristics of the soil, and the stiffness of the supporting structure all affect the greatest lateral deformation that a retaining wall can exhibit [11], and it usually happens next to the excavation surface [10]. The length of the wall significantly affects the failure mechanism's position, and the lateral wall's maximum deformation may be connected to Terzaghi's safety factor against basal heave [1], [2], [5]. This research investigates the horizontal deformation of the walls, the size and position of the ground surface settlement, and the principal effective stresses after excavation.

2. PLAXIS(2D) Modeling Program

2.1. Basic Information

Analysis of soil-structure interaction is performed using PLAXIS Version 8.6, which has 15 node components for modeling the soil continuum environment. With such a sizeable length-to-width ratio, a planar strain condition in two dimensions is anticipated for the station. There is a clear dichotomy between the layered characteristics of the soil's components. The ET(3) layer begins at the ground's surface and extends to a depth of 25 m, whereas the ET(2) layer begins at the surface and goes to a depth of 35 m (Table 1).

Table 1. Geotechnical characteristics of the station's materials

No	Layer	γ_{unsat} [KN/m^3]	γ_{sat} [KN/m^3]	C_{ref} [KN/m^2]	φ [◦]
1	ET(2)	18.4	20.0	15.0	33.0
2	ET(3)	19.0	20.0	30.0	33.0

2.2. Simulated Geometry and Mesh Generation

The geometry employed in this model has dimensions of around 120 meters in length and 60 meters in depth. The selected range is nearly equal to the depth of the supporting structures along the sides and below them. However, the model should not influence the outcomes within the model's scope. Drilled to a depth of 27 meters, the piles in this model have 18 m between their centers and are modeled using beam components. In addition, a four-row anchor element is modeled at 2,9,15, and 19 meters deep to stabilize and prevent lateral displacements. There is a contact between the soil and the peripheral piles; therefore, the interface elements are employed to simulate the interaction of soil structure. All ranges have meshed with 15 nodal elements, and the excavation region results in a finer mesh than other regions.

2.3. Loading and Boundary Conditions

A surface load of equals 50 (kN/m^2) has to be taken into consideration since there is an urban and residential development on both the south and the north sides of the excavation. The loading distance is 2m, starting at the excavation border and going to the end of the model. The boundary condition is considered to follow the fixity of the standard model. Consequently, the program will provide roller conditions along the vertical sides and complete fixity at the base geometry (Figure 1).

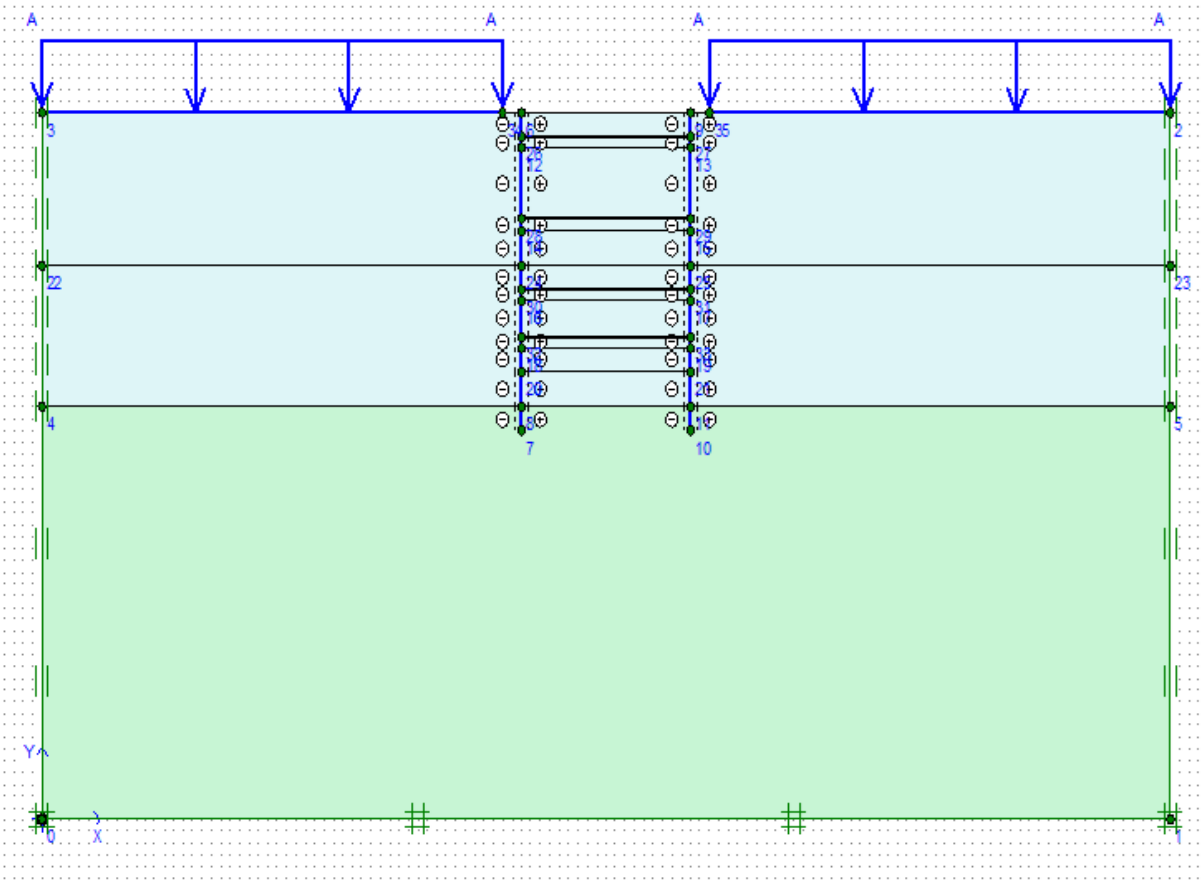

Figure 1. Finite element model in two dimensions: geometry, loading, and boundary conditions

2.4. Sets of Material

To replicate the properties of soil, the Hardening-Soil model is applied. This model captures the behavior of hyperbolic soil in general and its hardening in response to increased stress levels. In this model, the unloading modulus is different from the module loading. Due to the lack of unloading modulus of studies based on experiences in other soil, the unloading modulus is three times the intended load modulus. Plastic concrete piles with a 2.1 m diameter and a 2 m spacing were used to install the lateral walls forcibly, and the exact dimensions were used for the structurally overlapping piles. These walls are considered continuous and beam element models. Due to the distance of 2 m of the structural piles, the parameters of the beam element in modeling are half of the parameters corresponding to structural piles (EA and EI (model)) = 0.5 EA & EI (pile)). The distance between the middle struts is about 4 meters, and they are positioned at depths of 2, 9, 15, and 19 meters below the ground surface. These struts are kinds of hollow tube profiles. The outer diameter of the upper struts and their thickness are respectively 323.9 mm and 3.6 mm; the middle ones are 457.2 mm and 14.2 mm; the lower ones are 355.6 mm and 8mm. The parameters of walls and struts are in Tables 2 and 3, respectively.

Table 2. Lateral wall specifications

Name	Type	EA [KN/m]	EI [KN.m2/m]	W [KN/m2]	v
Diaphragm Wall	Elastic	1.19E7	1.07E6	13.50	0.2

Table 3. Struts parameters

ID	Name	EA [KN/m]	$F_{(max.comp)}$ [KN/m]	$F_{(max.tens)}$ [KN/m]
1	Upper Strut	4.587E5	2.50E14	2.50E14
2	Middle Struts	1.039E6	2.50E14	2.50E14
3	Lower Strut	5.722E5	2.50E14	2.50E14

2.5. Calculation

Eleven steps comprise the computation. Buildings to the south and north of the excavation provide initial stress in the first stage. This stage is before the excavation stage, and at the end of this stage, the beginning of the next stage, displacements are considered zero. The second step involves building the walls. During the third stage, three meters of the braced cut are dug out. The fourth stage involves setting up the upper struts. More digging to a depth of 10 meters is required in the fifth stage. The

installation of the middle struts in the structure's center is the task at hand during the sixth stage of the process. Extending the excavation depth to 16 meters is part of the seventh phase, as does dewatering the excavation. As part of the specification of the seventh step, this requires an analysis of groundwater flow to compute the new pore water distribution. Installation of the middle struts constitutes Stage eight. The ninth stage consists of dewatering the excavation site and continuing the excavation to a depth of twenty meters. The ninth stage involves the installation of the lower struts. In the last, eleventh stage, excavation is continued to a depth of 22 meters, and the site is dewatered.

3. Results and Discussion

Due to the excavation of the soil, the tension condition is changed and may cause some displacements and instabilities. As a result of this, the subsequent studies will describe the greatest horizontal and vertical displacements that occurred during excavation as well as the principal stresses that occurred after excavation.

3.1. Maximum Vertical and Horizontal Displacements

The vertical and horizontal displacements are increased with further excavation, and the location of the horizontal displacements is on the wall and near the depth of excavation (Figures 2 and 3). The maximum positive vertical displacements (heave) occur in the excavation depth, and the maximum negative vertical displacements occur under the ground surface. The maximum horizontal and positive vertical displacements are 35.32 and 35.00mm, respectively, and the maximum ground surface settlement is 22.41mm (Table 4).

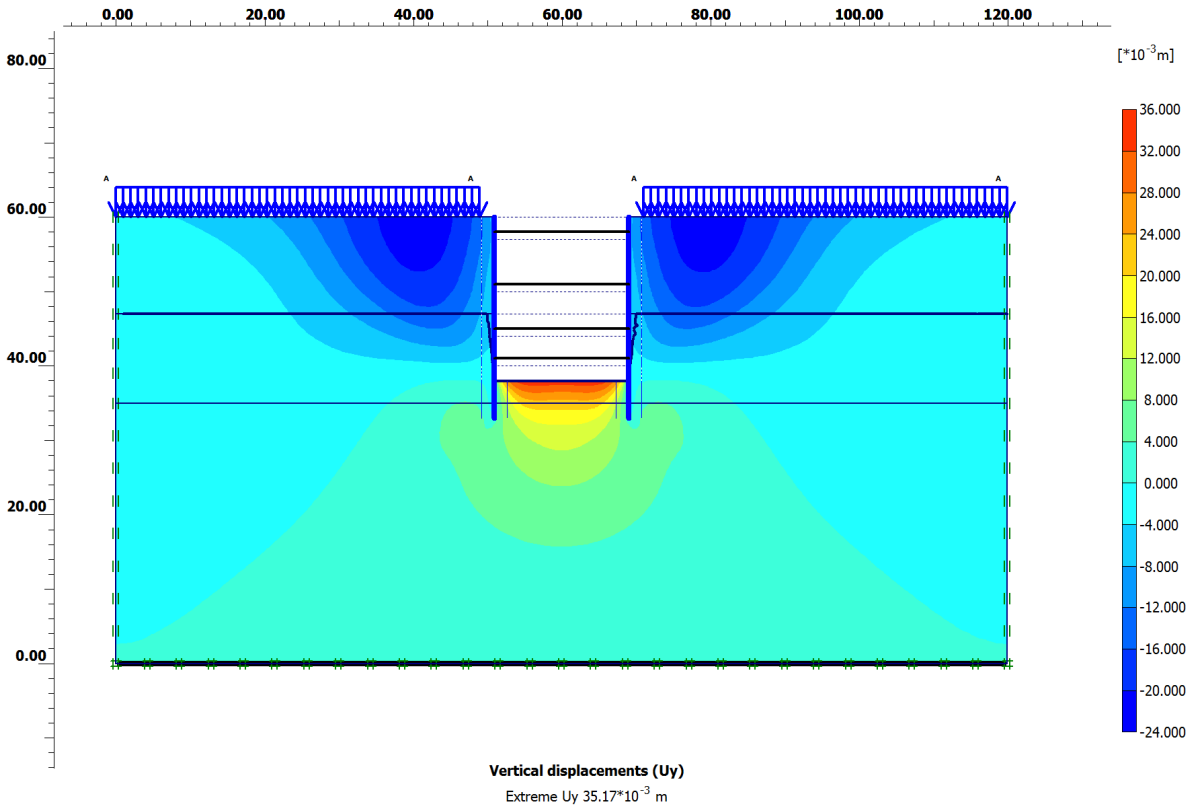

Figure 2. Vertical displacements shadings in the final stage

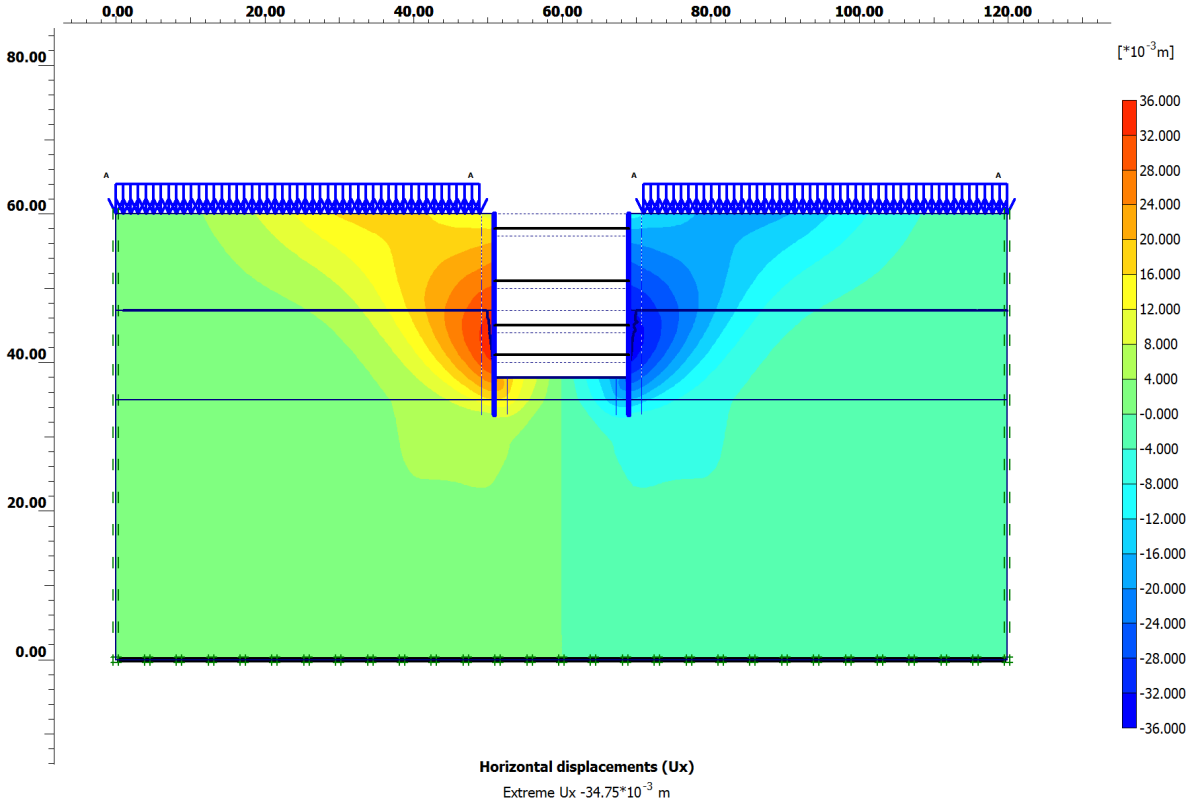

Figure 3. Horizontal displacements shadings in the final stage

Table 4. The maximum of the horizontal and vertical displacements

Phase Number	Horizontal (m)	Settlement(m)	Heave (m)
3	7.70E-04	-1.29E-03	4.76E-03
5	7.87E-03	-2.92E-03	1.97E-02
7	1.84E-02	-9.07E-03	2.78E-02
9	2.87E-02	-1.67E-02	3.23E-02
11	3.53E-02	-2.24E-02	3.50E-02

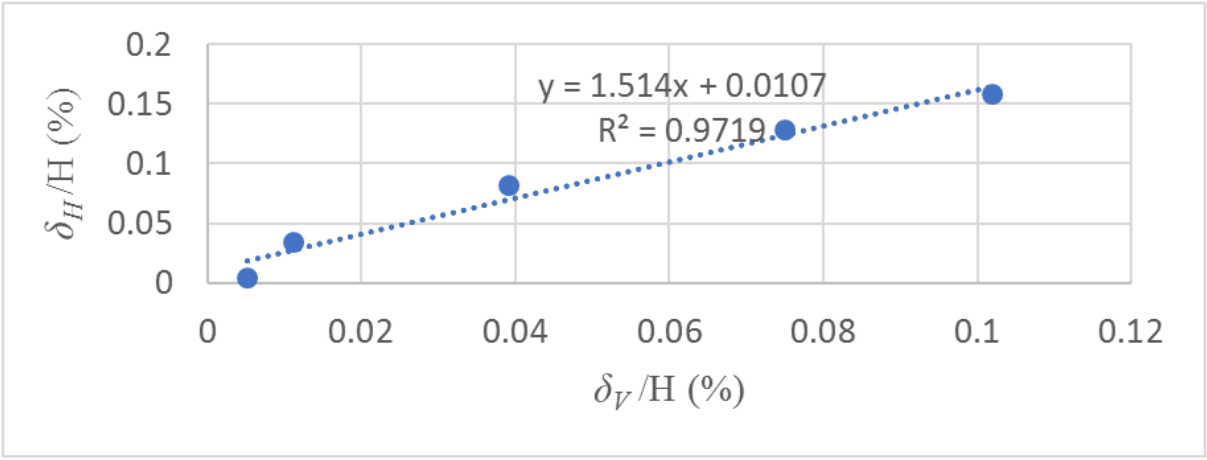

Figure 4. Relationship between the maximum ground surface settlement and lateral wall deflection

Figure 4 depicts the relationship between the maximum ground surface settlement and the maximum lateral wall deflection. In most excavation cases, the maximum lateral wall deflection, δ_H, is equal to $1.0\delta_V$ -$2.0\delta_V$ [10], [12]; in this case, this ratio reaches 1.5, where δ_V is the maximum ground surface settlement.

With further excavation, the deflection of the lateral wall increases. The maximum lateral displacement is seen in proximity to the excavation surface (Figure 5). There is a connection between the maximum deflection of a lateral wall and the excavation depth, which relies on the soil type and can be calculated as follows, which is less than Peck's (1969) data (0.01H) and Clough and O'Rourke's (1990) findings (0.002H) [10]:

$$\delta_{mH} = (0.00018 \sim 0.0016)\ H \quad (1)$$

where δ_{mH} and H are the maximum lateral wall deflection and the excavation depth, respectively.

Figure 6 shows different settlements of the ground surface in each phase. As we can see, further excavation causes more vertical displacements, especially after the fifth phase of excavating operation. On the other hand, these curves show that the maximum settlements on the ground happen near the excavation, which is related to the depth of excavation. The settlement effect zone is 51 meters from the excavation, which is more than Clough and O'Rourke's (1990) results for soft to medium clays, where the settlement influence zone is double the final excavation depth [9].

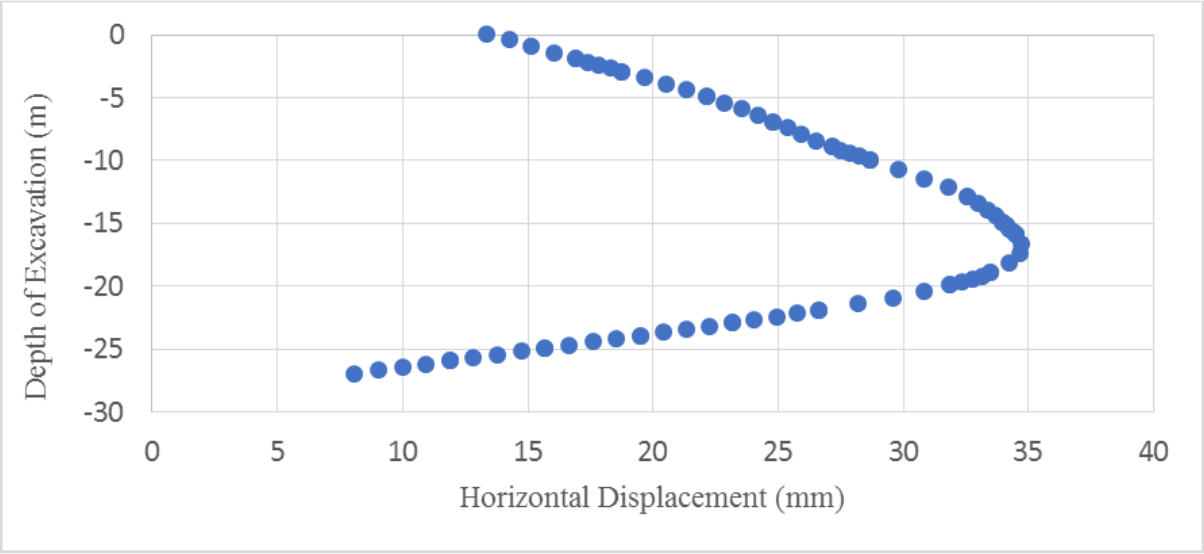

Figure 5. Last-stage lateral wall deflection during excavation

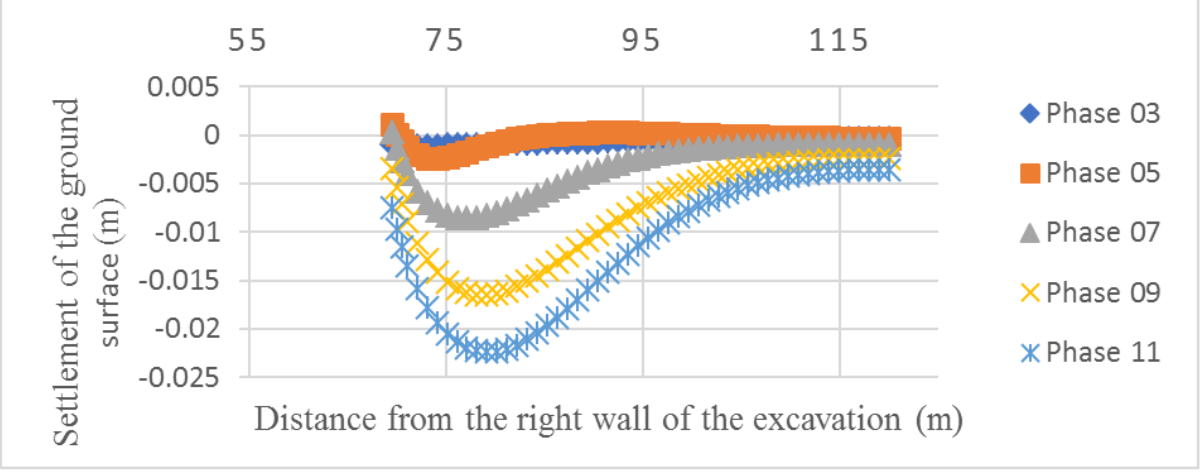

Figure 6. Relationship between the settlement of the ground surface with the distance from the excavation in different phases

Figure 7 illustrates the association between the maximum ground surface settlement locations and the excavation depths for all phases. The location of maximum ground surface settlement from the wall equals 0.4 times the excavation depth in each excavation phase, which is approximately equal to Ou et al. and Nicholson's findings [9], [10].

3.2. Principal Effective Stresses

With further excavation, the direction of the principal effective stresses is changed, and at the bottom of the excavation, the more significant principal stresses are horizontal, and the more minor principal stresses are vertical (Figure 8). Thus, the over-consolidation ratio increases during the excavation, reaching up to 3.41 (Figure 9). The effective horizontal stresses have grown in a great area at the bottom of the excavation, but shadings of the effective vertical stresses show a decrease in proportion to the vicinity (Figure 9).

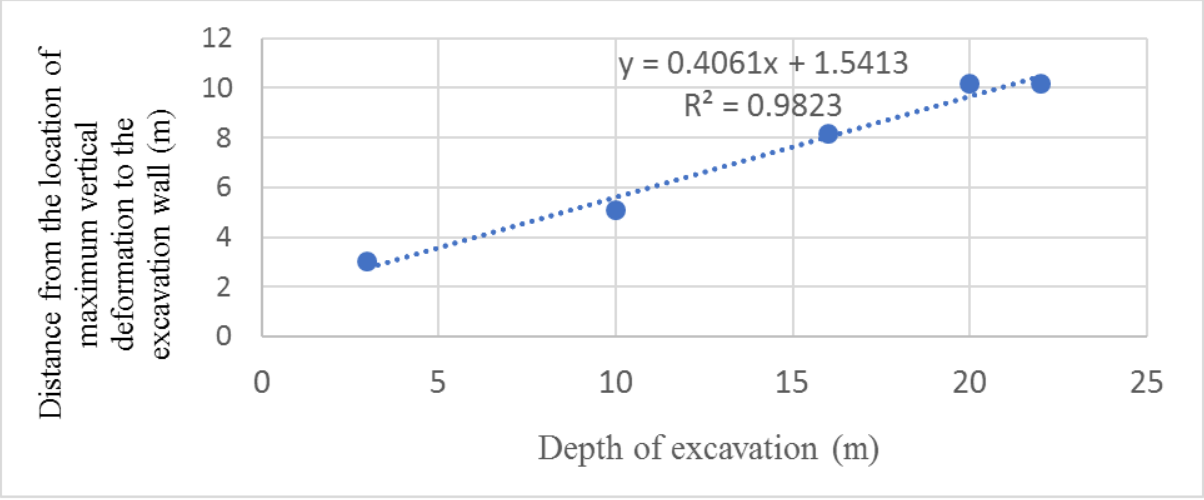

Figure 7. Relation between the location of maximum ground surface settlement and depth of excavation

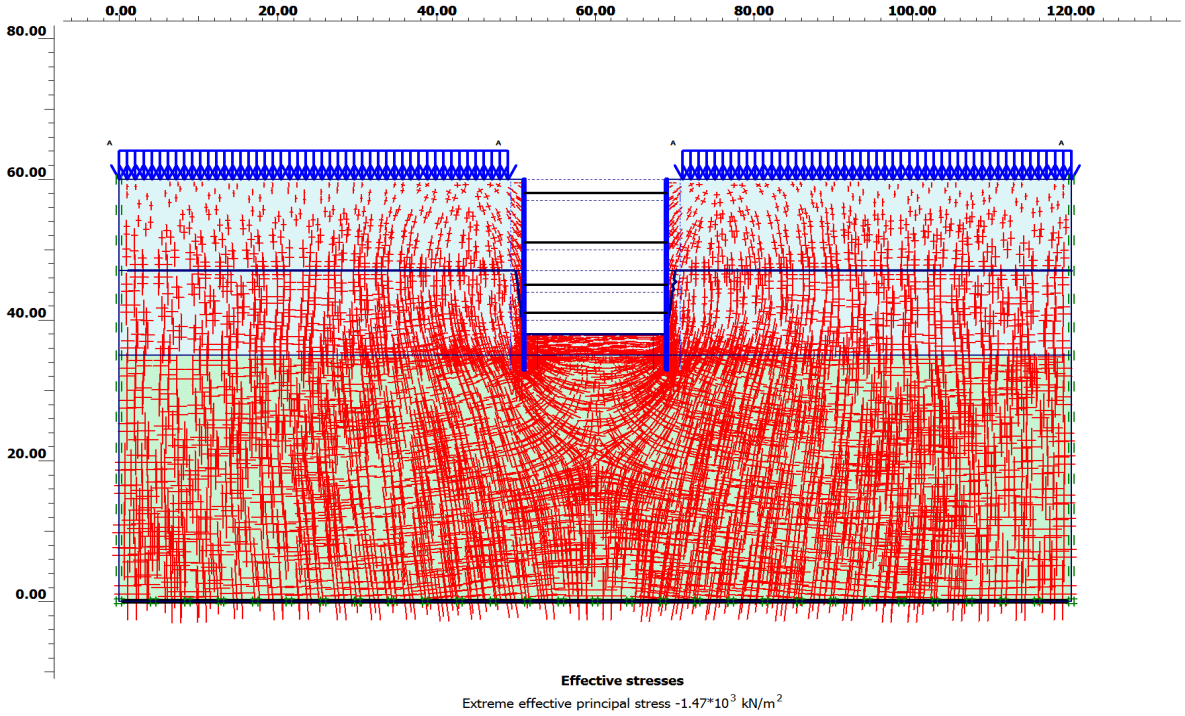

Figure 8. Principal stresses after excavation

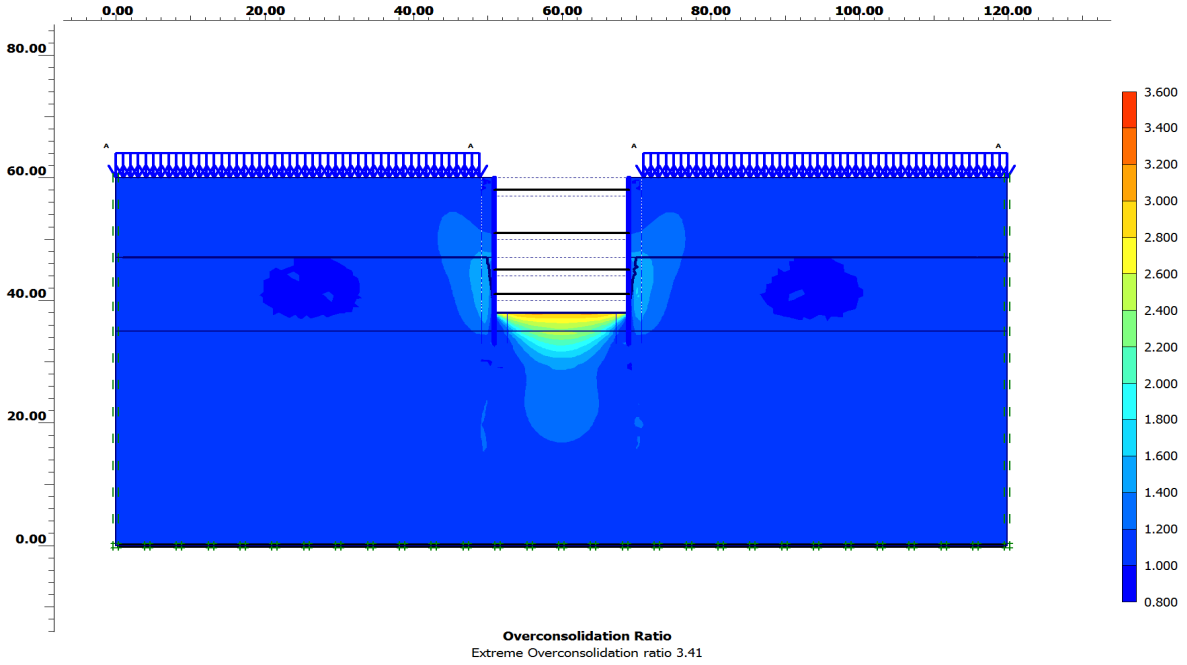

Figure 9. Over-consolidation ratio in the final stage

4. Conclusions

The impacts of excavation on ground surface settlement, lateral wall deflection, the connection between maximum lateral wall deflection and ground surface settlement in each phase, and the principal effective stresses were analyzed via the use of numerical analysis. The following conclusions were drawn based on this study:

- The most significant lateral wall displacement in all phases often occurred close to the excavation surface. The highest lateral wall displacement was between 0.00018H and 0.0016H; for the final stage, this value was 34.76 mm.
- There was a linear relationship between the maximum ground surface settlement and the maximum lateral wall deflection. In this case study, the lateral wall deflection was equal to 1.5 times the maximum ground surface settlement.
- The largest ground surface settling occurred near the wall face during the first excavation phase. However, the maximum ground surface settlement usually occurred at some distance from the wall for the subsequent phases. This distance did not vary with excavation depth. The settlement influence zone was about 51 m from the excavation, about 2.3 times the final excavation depth.
- In each excavation phase, the maximum ground surface settlement location was approximately 0.4 times the excavation depth, which was about equal to Ou et al. (1993) and Nicholson's (1987) findings.
- The direction of the principal effective stresses changed with further excavation. The effective horizontal stresses increased at the bottom of the excavation, while the effective vertical stresses decreased in proportion to the surrounding area.

5. Recommendation

The stress level in the soil changes as a consequence of excavation, and deformations and instability may develop. These deformations appear as lateral displacement in the walls of the braced cut, wall instability, swelling at the bottom of the cut (heave), and settlement in the surrounding areas.

The lateral movement of the piles may cause the surrounding ground surface to settle. The degree of lateral yield is determined by several variables, primarily the kind of soil at the bottom of the excavation. To significantly minimize the lateral yielding of the wall, piles should be driven to a depth below the excavation's bottom. However, the penetration depth will be useless if the clay underneath the excavation extends to a substantial depth and $\gamma H/c$ is around 8 (where γ, H, and c are the unit weight of clay, the height of the cut, and the undrained cohesion, respectively). If there is a hard clay layer at the excavation's bottom, the piles must penetrate it. This will significantly contribute to the reduction of lateral deformation.

Support systems must be created in extremely loose soils before excavation activities begin, but support systems may be erected step by step alongside excavation in reasonably stable soils. It should be mentioned that many soils contain a safety factor that may decrease with time depending on the circumstances of their types and component minerals. In urban excavations, due to the limited geometry of the land, the difficulty of

implementation, ensuring the comfort of neighbors, not causing damage to nearby buildings, the presence of vital urban arteries, and the inability to use specific equipment, methods of ensuring stability, reducing deformations, and the settlement of the surrounding lands must be selected with greater care. In this approach, classical methods (execution of horizontal struts) or modern methods such as soil reinforcement (reinforced construction with belts and all types of geogrids and geotextiles) are used in conjunction with moving the soil or nailing the wall without moving the soil.

Funding

This research was funded by Universiti Putra Malaysia (GP-IPS/2016/95032).

REFERENCES

[1] R. J. Finno and J. F. Roboski, "Three-Dimensional Responses of a Tied-Back Excavation through Clay," J. Geotech. Geoenvironmental Eng., vol. 131, no. 3, pp. 273–282, 2005, doi:10.1061/(ASCE)1090-0241(2005)131:3(273).

[2] J. H. Wang, Z. H. Xu, and W. D. Wang, "Wall and Ground Movements due to Deep Excavations in Shanghai Soft Soils," *J. Geotech. Geoenvironmental Eng.*, vol. 136, no. 7, pp. 985–994, 2009, doi:10.1061/(ASCE)GT.1943-5606.0000299.

[3] R. J. Finno, J. T. Blackburn, and J. F. Roboski, "Three-Dimensional Effects for Supported Excavations in Clay," *J. Geotech. Geoenvironmental Eng.*, vol. 133, no. 1, pp. 30–36, 2007, doi: 10.1061/(ASCE)1090-0241(2007)133:1(30).

[4] G. T. C. Kung, C. Y. Ou, and C. H. Juang, "Modeling small-strain behavior of Taipei clays for finite element analysis of braced excavations," *Comput. Geotech.*, vol. 36, no. 1–2, pp. 304–319, 2009, doi: 10.1016/j.compgeo.2008.01.007.

[5] Y. M. a. Hashash and A. J. Whittle, "Ground Movement Prediction for Deep Excavations in Soft Clay," *J. Geotech. Eng.*, vol. 122, no. 6, pp. 474–486, 1996, doi: 10.1061/(ASCE)0733-9410(1996)122:6(474).

[6] J. Tanner Blackburn and R. J. Finno, "Three-Dimensional Responses Observed in an Internally Braced Excavation in Soft Clay," *J. Geotech. Geoenvironmental Eng.*, vol. 133, no. 11, pp. 1364–1373, 2007, doi: 10.1061/(ASCE)1090-0241(2007)133:11(1364).

[7] R. J. Finno, I. S. Harahap, P. J. Sabatini, and F. Molenkamp, "Analysis of braced excavations with coupled finite element formulations," *Comput. Geotech.*, vol. 12, no. 2, pp. 91–114, 1991, doi: http://dx.doi.org/10.1016/0266-352X(91)90001-V.

[8] A. Whittle, Y. Hashash, and R. Whitman, "Analysis of Deep Excavation in Boston," *J. Geotech. Eng.*, vol. 119, no. 1, pp. 69–90, Jan. 1993, doi: 10.1061/(ASCE)0733-9410(1993)119:1(69).

[9] P.-G. Hsieh and C.-Y. Ou, "Shape of ground surface settlement profiles caused by excavation," *Can. Geotech. J.*, vol. 35, no. 6, pp. 1004–1017, 1998, doi: 10.1139/t98-056.

[10] C.-Y. Ou, P.-G. Hsieh, and D.-C. Chiou, "Characteristics of ground surface settlement during excavation," *Can. Geotech. J.*, vol. 30, no. 5, pp. 758–767, 1993, doi: 10.1139/t93-068.

[11] L. Mu and M. Huang, "Small strain based method for predicting three-dimensional soil displacements induced by braced excavation," *Tunn. Undergr. Sp. Technol.*, vol. 52, pp. 12–22, 2016, doi: 10.1016/j.tust.2015.11.001.

[12] B.-C. B. Hsiung, "A case study on the behaviour of a deep excavation in sand," *Comput. Geotech.*, vol. 36, no. 4, pp. 665–675, 2009, doi: 10.1016/j.compgeo.2008.10.003.